ACS APPLIED MATERIALS & INTERFACES

Research Article

www.acsami.org

Conjugated Polymer Energy Level Shifts in Lithium-Ion Battery Electrolytes

Charles Kiseok Song,[†,∥] Brian J. Eckstein,[†,∥] Teck Lip Dexter Tam,[†] Lynn Trahey,*[,‡] and Tobin J. Marks*[,†,§]

[†]Department of Chemistry, Northwestern University, 2145 Sheridan Road, Evanston, Illinois 60208, United States

[‡]Chemical Sciences and Engineering Division, Argonne National Laboratory, Argonne, Illinois 60439, United States

[§]Department of Materials Science and Engineering, Northwestern University, 2220 Campus Drive, Cook Hall Room 2036, Evanston, Illinois 60208, United States

Supporting Information

ABSTRACT: The ionization potentials (IPs) and electron affinities (EAs) of widely used conjugated polymers are evaluated by cyclic voltammetry (CV) in conventional electrochemical and lithium-ion battery media, and also by ultraviolet photoelectron spectroscopy (UPS) in vacuo. By comparing the data obtained in the different systems, it is found that the IPs of the conjugated polymer films determined by conventional CV (IP_C) can be correlated with UPS-measured HOMO energy levels ($E_{H,UPS}$) by the relationship $E_{H,UPS} = (1.14 \pm 0.23) \times qIP_C + (4.62 \pm 0.10)$ eV, where q is the electron charge. It is also found that the EAs of the conjugated polymer films measured via CV in conventional (EA_C) and Li^+ battery (EA_B) media can be linearly correlated by the relationship $EA_B = (1.07 \pm 0.13) \times EA_C + (2.84 \pm 0.22)$ V. The slopes and intercepts of these equations can be correlated with the dielectric constants of the polymer film environments and the redox potentials of the reference electrodes, as modified by the surrounding electrolyte, respectively.

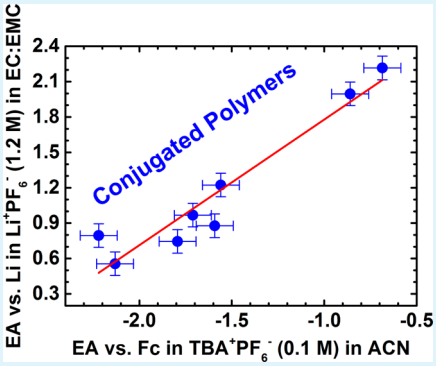

KEYWORDS: *lithium-ion battery, conjugated polymer, electron affinity, cyclic voltammetry, electrolyte, organic photovoltaics*

INTRODUCTION

Conjugated polymers find use in numerous electronics applications because of their exceptional properties, which include mechanical flexibility, production scalability, and chemically tunable electrical/electronic properties.[1−4] These materials have been successfully implemented in organic photovoltaic cells,[5−8] organic light-emitting diodes,[9−12] and organic transistors.[13,14] Recently, conjugated polymers have also been employed in lithium-ion battery (LIB) applications to replace[15−17] and/or enhance conventional carbon-based electrodes,[18−20] and significantly enhanced battery performance has been reported.

The LIB is a widely used energy storage system with applications that range from portable appliances to automobiles.[21,22] An important LIB figure-of-merit is the specific capacity.[23] One way to increase overall LIB capacity is to replace the ubiquitous carbon anode with one based on Si or Sn, which offer theoretical specific capacities of 4200 and 994 mAh/g, respectively, far surpassing that of graphite, 372 mAh/g.[24,25] The principal challenge facing Si and Sn battery anode technologies is managing the up to 320% volumetric expansion/contraction of the anode during Li_xM intermetallic formation in the charge/discharge processes.[25] Repeated expansion and contraction cause destructive anode fragmentation, exposing fresh anode surfaces to the organic electrolyte. These electrolyte materials readily undergo chemical reduction on the electrode surfaces, yielding passivating solid−electrolyte interface (SEI) films that irreversibly consume the Li^+ ions essential for energy storage.[26−29] For these reasons, active research efforts have focused on developing protective materials systems based on conjugated polymers to minimize cycling-induced anode damage.[17−20]

Note that the electrochemical properties of polymers potentially useful for battery applications must be characterized in depth for the relevant electrochemical environment of use. Specifically, quantifying the energetics of the highest occupied molecular orbital (HOMO) and lowest unoccupied molecular orbital (LUMO) are essential to understanding the aforementioned electrochemical properties. The conjugated polymer LUMO energy is especially important since it relates to charge transport and stability at the anode;[18,19] and when the anode potential coincides with the polymer LUMO energy, the reduction of Li^+ to Li occurs and SEI films form.[23,27,28] However, note that conjugated polymer energy levels are typically derived from electrochemical measurements performed in completely different electrolyte environments than

Received: August 13, 2014
Accepted: October 20, 2014
Published: October 20, 2014

Scheme 1. Conjugated Polymers Used in This Study[a]

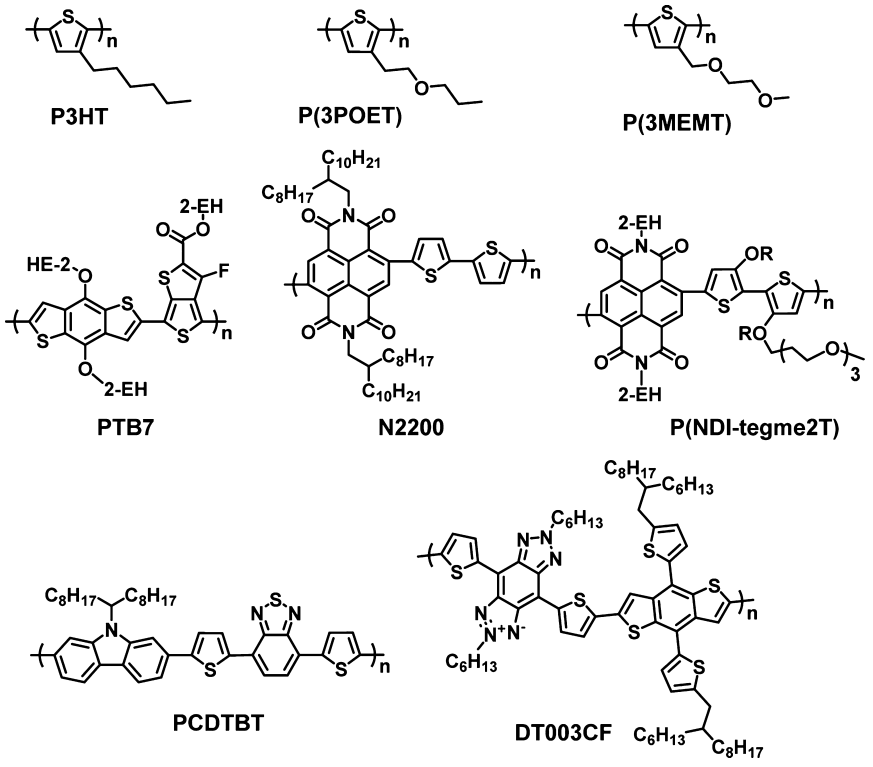

[a]2-EH = 2-ethylhexyl.

Table 1. Cyclic Voltammetry Experimental Parameters and Terminologies

experimental detail	conventional system (CV_C)	battery system (CV_B)
working electrode	Pt (0.20 cm^2)	patterned glass/Cu (0.50 cm^2)
reference electrode	Ag/AgCl (aq) in KCl (3.0 M)	Li
counter electrode	Pt	Li
electrolyte (conc.)	$TBA^+PF_6^-$ (0.1 M)	$Li^+PF_6^-$ (1.2 M)
solvent	acetonitrile, anhydrous	EC:EMC (3:7)
scan rate	100 mV/s	10 mV/s
sweep range	−2300 to 2300 mV	10−3300 mV
LUMO labeling (CV/absolute scale)	$EA_C/E_{L,C}$	$EA_B/E_{L,B}$
HOMO labeling (CV/absolute scale)	$IP_C/E_{H,C}$	$IP_B/E_{H,B}$

the commonly used LIB liquid carbonate battery electrolytes. Conjugated polymer thin films are conventionally characterized in moderately polar organic solvents such as acetonitrile with ∼0.1 M organic salt as the electrolyte. In contrast, LIBs typically utilize high $Li^+PF_6^-$ electrolyte concentrations (∼1.2 M) in mixtures of very polar solvents such as ethylene carbonate (EC) + ethyl methyl carbonate (EMC). Therefore, the frontier orbital energies of conjugated polymers of potential interest could, in principal, shift from those measured in conventional and LIB electrochemical media when estimated by cyclic voltammetry (CV).

In this study, we quantify the frontier orbital energetics of a selected series of known and new conjugated polymers in LIB media and in conventional electrochemical media. To quantify HOMO energies without the intrusion of electrochemical medium effects, in vacuo ultraviolet photoelectron spectroscopy (UPS) is also applied since this alternative method is commonly used to characterize the electronic structure of conjugated polymers.[30−32] The conjugated polymers characterized in this study are P3HT, poly(3-(2-propoxyethyl)-thiophene) (P(3POET)), poly(3-((2-methoxy-ethoxy)methyl)-thiophene) (P(3MEMT)), poly[[4,8-bis[(2-ethylhexyl)oxy]-benzo[1,2-*b*:4,5-*b*′]dithiophene-2,6-diyl][3-fluoro-2-[(2-ethylhexyl)carbonyl]thieno[3,4-*b*]thio-phenediyl]] (PTB7), poly[*N*-9′-heptadecanyl-2,7-carbazole-*alt*-5,5-(4′,7′-di-2-thienyl-2′,1′,3′-benzothia-diazole)] (PCDTBT), poly[(5,5′-(4,8-bis-(thien-2-yl))-2,6-(dihexyl)benzo[1,2-*d*;4,5-*d*′]bis[1,2,3]-triazole-*alt*-(4,8-bis(5-(2-hexyldecyl)thien-2-yl)benzo[1,2-*b*:4,5-*b*′]dithien-2-yl)] (DT003CF), ActiveInk N2200 (Polyera Corp.), and poly(2,7-(*N*,*N*′-bis(2-ethylhexyl)-naphthalene-diimide)-*co*-5,5′-(3,3′-bis(2-(2-(2-methoxyethoxy)-ethoxy)-ethoxy)-2,2′-bithiophene)) (P(NDI-tegme2T)). The molecular structures are shown in Scheme 1. We report here that the estimated orbital energies of these conjugated polymers differ substantially with measurement technique, but also that informative predictive correlations exist between energies measured by UPS, conventional CV, and CV in a commonly used battery medium.

Regarding experimental data, the ionization potentials (IPs), electron affinities (EAs), HOMO energies (E_H's), and LUMO

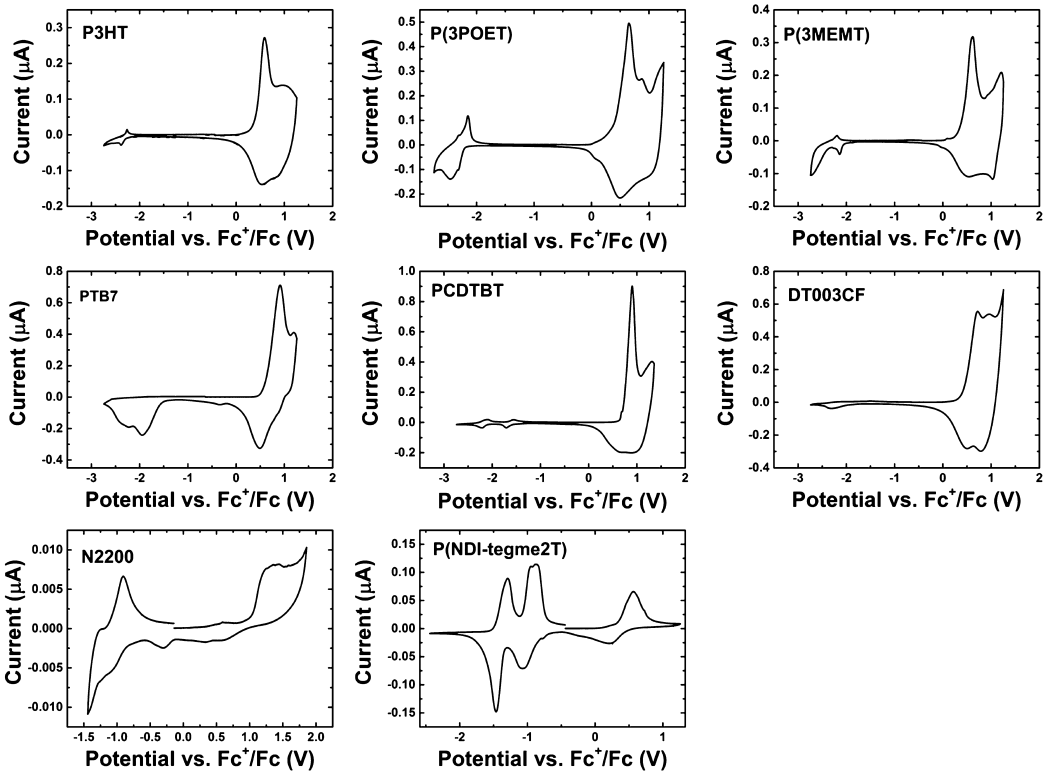

Figure 1. CV scans of conjugated polymer films in 0.1 M $TBA^+PF_6^-$ in anhydrous acetonitrile. Positive and negative currents represent oxidation and reduction, respectively.

Table 2. Solution-Phase Electrochemical Data

polymer	IP_C vs E_{Fc} (V)[a]	EA_C vs E_{Fc} (V)[a]	$E_{H,C}$ (eV)[b]	$E_{L,C}$ (eV)[c]	literature $E_{H,C}/E_{L,C}$ (eV)[d]	ref
P3HT	0.032	−2.13	5.13	2.97	4.75/2.73	34
P(3POET)	−0.036	−2.22	5.06	2.88	NA	
P(3MEMT)	0.075	−1.79	5.13	3.31	5.13/NA	35
PTB7	0.480	−1.56	5.58	3.54	5.55/3.40	8
PCDTBT	0.649	−1.59	5.75	3.51	5.65/3.48	36
DT003CF	0.342	−1.71	5.44	3.39	NA	
N2200	0.833	−0.86	5.93	4.24	5.97/4.32	37
P(NDI-tegme2T)	0.076	−0.69	5.18	4.41	NA	

[a]Estimated uncertainty range is 0.1 V. [b]Calculated from eq 1. [c]Calculated from eq 2. [d]Data reprocessed according to eqs 1 and 2.

energies (E_L's) determined by conventional CV (CV_C),[33,34] by CV in a battery medium (CV_B), and by UPS are first acquired and compared; all energy levels are reported on the corresponding absolute scale. Then, a brief discussion of the origin of the energy level shifts and apparent correlations follows. To aid in comparing data from different measurements, abbreviations and experimental details are summarized in Table 1. Details of experimental procedures and conditions are described in the Supporting Information.

RESULTS AND DISCUSSION

Cyclic Voltammetry with Conventional Electrolytes/Electrodes. CV scans in 0.1 M $TBA^+PF_6^-$/acetonitrile yield IP_C (ionization potential in conventional medium) and EA_C (electron affinity in conventional medium) data for the conjugated polymer series of this study, which are shown in Figure 1. The CV scans exhibit oxidation and reduction peaks with positive and negative currents, respectively, and peak onsets are found in the ranges of −0.32 to 1.03 V and −2.22 to −0.69 V versus Fc^+/Fc, respectively. These potentials are next converted to HOMO and LUMO energies with respect to the vacuum level using well-known eqs 1 and 2.[35,36] Here, $E_{H,C}$ and $E_{L,C}$ represent the HOMO and LUMO energies, respectively, and IP_C and EA_C are the onsets of the

$$E_{H,C} = qIP_C + 5.1\ \text{eV} \quad (1)$$

$$E_{L,C} = qEA_C + 5.1\ \text{eV} \quad (2)$$

polymer oxidation and reduction peaks versus Fc^+/Fc, respectively, and q is the electron charge. The 5.1 eV is the commonly used conversion factor to relate the Fc redox couple formal potential (E_{Fc} = 0.630 V vs NHE[37]) to an absolute scale (E_{NHE} = 4.5 eV).[38] Although there is some literature discussion regarding the accuracy of this approximation, which does not rigorously account for the measurement phase (vacuum vs liquid),[36] it pragmatically places the relevant energy levels on an absolute scale.[36] Since there are several variants of eqs 1 and 2, the previously reported orbital energies of P3HT,[39] P(3MEMT),[40] PTB7,[8] PCDTBT,[41] and N2200[42] are recalibrated here to eqs 1 and 2 and are compared to values

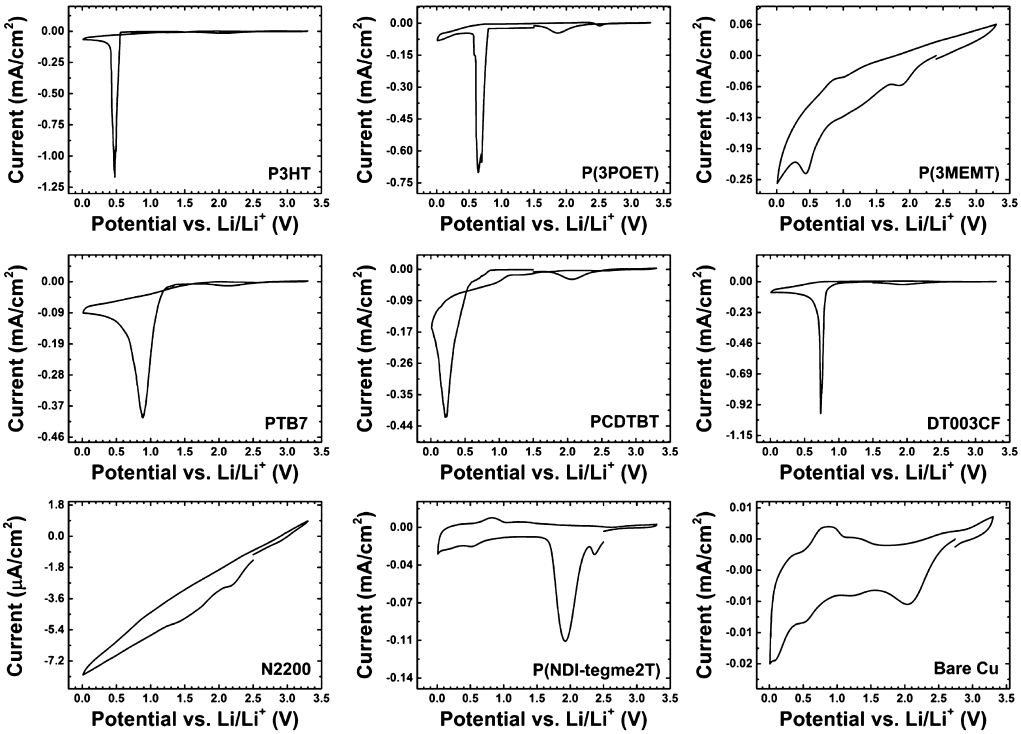

Figure 2. CV scans of conjugated polymer films in 1.2 M $Li^+PF_6^-$ in 3:7 EC:EMC. Positive and negative currents represent oxidation and reduction, respectively.

determined in the present study in Table 2. Note that the current values generally track those in the literature. These data are also compared to UPS data to assess the validity of eqs 1 and 2, as discussed below. The onsets of the oxidation and reduction peaks along with the corresponding energy levels on the absolute scale from eqs 1 and 2 are summarized in Table 2.

Cyclic Voltammetry with a Battery Electrolyte/Electrode System. The first CV scans from a three-electrode system in 1.2 M $Li^+PF_6^-$/3:7 EC:EMC yield the EA_B (electron affinity in battery medium) values of the conjugated polymers (Figure 2). After a complete scan, all of the present polymer films are visually bleached except N2200 and P(NDI-tegme2T). Note that $IP_B/E_{H,B}$ values (ionization potential/HOMO energy in battery medium) could not be obtained here due to competing Cu electrode oxidation (IP_B of Cu ~ 3.4 V vs E_{Li}). Also, the EA_B's of several polymers could not be observed, presumably because their high-lying LUMOs lie beyond the Li plating potential (~0.0 V vs E_{Li}). Thus, only data for polymers with reproducibly measurable EA_B values are reported. Next, eq 2 was modified by replacing E_{Fc} with the work function of Li (Φ_{Li} = 2.49 eV[43]), as in eq 3, and polymer $E_{L,B}$ values on an absolute scale estimated. This yields $E_{L,B}$ values

$$E_{L,B} = qEA_B + 2.49\ \text{eV} \quad (3)$$

(LUMO energies in battery medium) close to $E_{L,C}$; however, some discrepancies are apparent, the origins of which are discussed below. CV data and energy differences ($\Delta E_L = E_{L,C} - E_{L,B}$) are summarized in Table 3.

UPS and CV Correlations. UPS data (Figure S2, Supporting Information were used to derive $E_{H,UPS}$ (HOMO energy in vacuo) from the work function (Φ_s) and the valence band maximum (VBM) values of the conjugated polymers on Cu foil. Here, Φ_s is determined from the averaged spectra of four measurements using the difference between the secondary

Table 3. Cylic Voltammetry Data in Battery Medium

polymer	EA_B vs E_{Li} (V)[a]	$E_{L,B}$ (eV)[b]	ΔE_L (eV)
P3HT	0.56	3.05	−0.08
P(3POET)	0.79	3.28	−0.40
P(3MEMT)	0.75	3.24	−0.33
PTB7	1.22	3.71	−0.17
PCDTBT	0.88	3.37	0.14
DT003CF	0.97	3.46	−0.07
N2200	2.00	4.49	−0.25
P(NDI-tegme2T)	2.22	4.71	−0.30

[a]Estimated uncertainty range is 0.1 V. [b]Calculated value from eq 3.

electron cutoff (SECO), the highest binding energy, and the He I source energy (21.22 eV).[44,45] The VBM values of the polymer-coated Cu foils relative to the Fermi level (0.0 eV) were determined from the onset of the lowest binding energy. The IP, or $E_{H,UPS}$, was then calculated from the sum of Φ_s and the VBM.[44,46] Note that the UPS-derived $E_{H,UPS}$ values track the $E_{H,C}$'s closely, but some discrepancies ($\Delta E_H = E_{H,C} - E_{H,UPS}$) as large as 0.72 eV are found (Table 4). However, ΔE_H

Table 4. UPS Data Summary

polymer	$E_{H,UPS}$ (eV)[a]	ΔE_H (eV)	$E_{H,C,cor}/\Delta E_{H,cor}$ (eV)[b]
P3HT	4.52	0.61	4.66/0.14
P(3POET)	4.73	0.34	4.58/−0.15
P(3MEMT)	4.78	0.35	4.65/−0.13
PTB7	5.07	0.51	5.17/0.10
PCDTBT	5.24	0.51	5.36/0.12
DT003CF	4.73	0.72	5.01/0.29
N2200	5.84	0.09	5.57/−0.27
P(NDI-tegme2T)	4.81	0.36	4.71/−0.11

[a]The estimated error range is 0.1 V. [b]Calculated value from eq 4.

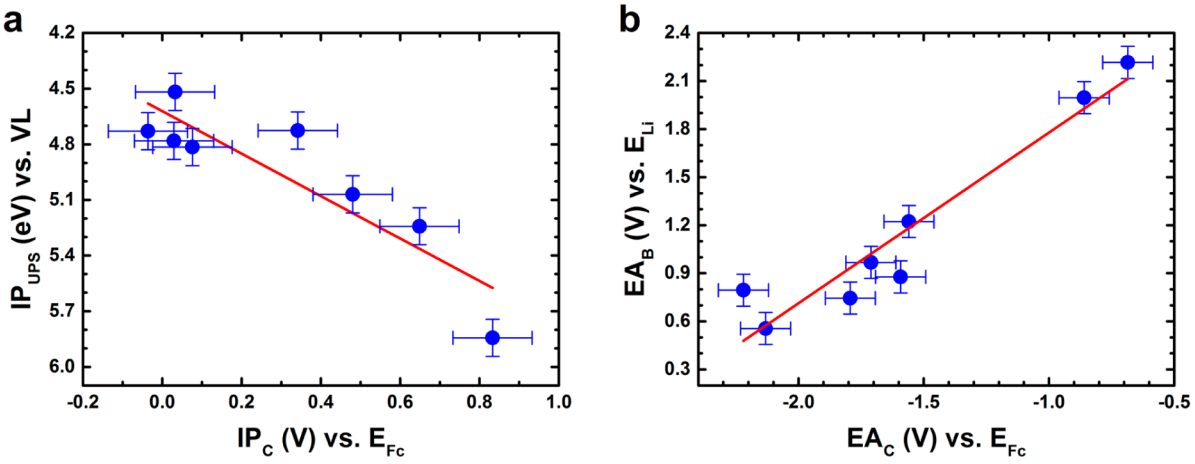

Figure 3. (a) IP_{UPS} plotted against IP_C and (b) EA_B plotted against EA_C for the present series of polymers. For (a), the best linear fit (R^2 = 0.76) has a slope of 1.14 ± 0.24 and an intercept of 4.62 ± 0.10. For (b), the best linear fit (R^2 = 0.90) has a slope of 1.07 ± 0.13 and an intercept of 2.84 ± 0.22. Red straight line indicates the best linear fit.

is significantly reduced ($\Delta E_{H,cor}$) when the correction suggested by D'Andrade[35] (eq 4) is applied instead of eq 1.

$$E_{H,C,cor} = (1.4 \pm 0.1) \times qIP_C + (4.6 \pm 0.08)\ \text{eV} \quad (4)$$

In this model, $E_{H,C,cor}$ denotes the corrected $E_{H,C}$ value, and the slope of eq 4 reflects analyte image charge and solvation effects on the electrode surface interacting with the surrounding electrolyte, and the intercept of 4.6 is the Φ_s of ferrocene. D'Andrade argued that the image charges induced by an analyte on a conductive surface under vacuum or in a polar solvent skew the energy level correlation from unity. In general, the greater the image charge, the greater the slope, with the image charge directly proportional to the dipolar strength of the charged analyte. In the present study, a relationship similar to eq 4 (eq 5) is obtained by plotting IP_C vs IP_{UPS} (Figure 3a).

$$E_{H,C,\,cor} = (1.14 \pm 0.23) \times qIP_C + (4.62 \pm 0.10)\ \text{eV} \quad (5)$$

The principal factors contributing to the disparities in the results of this investigation and D'Andrade's model are the analyte solvation effects. D'Andrade et al. used small molecule analytes dissolved in the electrolyte for CV measurements, minimizing interanalyte molecule/ion interactions and maximizing electrolyte solvation. In the present study, CV is performed on solid thin films where solvation effects should be far less, but in which interanalyte interactions should be large. However, as D'Andrade et al. note, solvation effects should be small compared to the image charge effects for adsorbed analytes,[35] contributing to the similarity of eqs 4 and 5. Note that UPS measurements are on analyte films cast on metal electrodes; thus, any disparities between eqs 4 and 5 should not originate from the forms of the UPS samples.

$EA_C - EA_B$ Correlations. For the same conjugated polymer, the orbital energies obtained from CV_C and CV_B are clearly different and likely reflect the different reference electrodes employed (Fc^+/Fc vs Li^+/Li). Furthermore, the frontier orbital energetics of the conjugated polymers are expected to vary with solvent and electrolyte concentration. If the origin of these differences is ascribed solely to the reference electrode, the analyte energy levels should uniformly shift with the potential differences of the reference electrodes. However, when EA_C and EA_B data are compared, the differences are significantly smaller than the reference electrode potential difference ($E_{Fc} - E_{Li}$ = 3.675 V), and other sources of energy level shifts, such as electrolyte concentration[47−49] and solvation, must be considered.[50−52] Classic examples of this effect include the EA shift of Tl^+ (~0.2 V) with increasing electrolyte concentration of 0.1 to 100 mM,[47] and the O_2 IP shift of 0.31 V at a Pt electrode on changing the solvent from DMSO to acetonitrile.[51] In the present case, CV_C and CV_B measurements are conducted in 0.1 M $TBA^+PF_6^-$/acetonitrile and 1.2 M $Li^+PF_6^-$/EC:EMC, respectively, corresponding to a large change in electrochemical environment.

Similar to D'Andrade's approach,[35] the EA_C and EA_B data for the present polymers are plotted against each other in Figure 3b. A reasonable linear correlation (R^2 = 0.90) is observed, indicating that the orbital energetics from one measurement are approximately translatable to the other within the −2.4 to −0.4 V range. Thus, EAs of conjugated polymers in a battery medium can be estimated ($EA_{B,est}$) from CV_C measurements using eq 6. The parameters in this equation

$$EA_{B,est} = (1.07 \pm 0.13) \times EA_C + (2.84 \pm 0.22)\ \text{V} \quad (6)$$

afford insights into the relevant electrochemical phenomena in that the intercept (2.84 ± 0.22 V) is less than the reference electrode potential difference (3.675 V), but the slope is near unity, implying that conjugated polymers measured as thin films on electrodes by CV_C and CV_B experience minimal differential solvation effects. However, note that the slope is greater than unity when UPS and CV_C data are compared. D'Andrade modeled such slopes by the ratio of the dielectric constants of the respective analyte media. The medium in D'Andrade's model is the neighboring analyte in films for UPS, and electrolyte in CV—hence, the dielectric constant differences are very large. In the present case, the analyte is not likely to be extensively solvated but embedded in a solid film in both CV experiments. Thus, dielectric constant effects in this model should be relatively small and a slope near unity is expected—exactly what eq 6 reveals. Thus, the apparent orbital energy shifts primarily arise from the potential difference between the reference electrodes; however, as noted above, the electrochemical potentials are also affected by the electrolyte concentration,[47,48] solvation,[51,52] and image charge effects, which alter the working electrode potential, as well as that of the reference electrode.[35,53,54] Indeed, E_{Fc} on the absolute electrochemical scale is 5.1 eV, while Φ_{Fc} = 4.6 eV. Similarly, E_{Li}

dx.doi.org/10.1021/am505416m | ACS Appl. Mater. Interfaces 2014, 6, 19347−19354

on the absolute scale is 1.44 eV, but Φ_{Li} = 2.49 eV, where the differences likely originate from reference electrode−electrolyte interactions. A similar phenomenon is also observed with the SHE.[55−57] These results signify that simple addition/subtraction of a single parameter to convert orbital energies in one electrochemical environment to another can introduce significant errors. Note also that some polymers do not strictly follow the linear trend in Figure 3. This phenomenon may arise from differences in the polymer−electrolyte interactions; however, further studies will be required to better define these interactions.

CONCLUSIONS

The orbital energetics of a series of established conjugated polymers were analyzed by CV in conventional and Li-ion battery solution environments, and by UPS in vacuo. By comparing data obtained from these two regimes, it is seen that the ionization potentials measured by conventional CV can be correlated with the UPS-derived HOMO energies via $E_{H,C,corr}$ = (1.14 ± 0.23) × qIP$_C$ + (4.62 ± 0.10) (eV) and the electron affinities of conjugated polymers measured by CV in conventional and Li^+ battery environments can be linearly correlated by the relationship $EA_{B,est}$ = (1.07 ± 0.13) × EA_C + (2.84 ± 0.22) (eV). The slopes and the intercepts of these equations are related to the dielectric constants of the analyte environments and the redox potentials of the reference electrodes as affected by the surrounding electrolyte, respectively. We expect that the correlations and their origins described here will be useful in analyzing/predicting the electronic structures of diverse conjugated polymers being considered for organic electronic and energy storage applications.

ASSOCIATED CONTENT

Supporting Information

More details of polymer synthesis, CV and UPS experimental methods, and data of the conjugated polymers are described. This material is available free of charge via the Internet at http://pubs.acs.org.

AUTHOR INFORMATION

Corresponding Authors

*E-mail: trahey@anl.gov (L.T).
*E-mail: t-marks@northwestern.edu (T.J.M.).

Author Contributions

‖These authors contributed equally to this work.

Notes

The authors declare no competing financial interest.

ACKNOWLEDGMENTS

This research was supported in part by the Institute for Sustainability and Energy at Northwestern (ISEN) (C.K.S.) and by the Argonne-Northwestern Solar Energy Research (ANSER) Center, an Energy Frontier Research Center funded by the U.S. Department of Energy, Office of Science, Office of Basic Energy Sciences, under Award Number DE-SC0001059 (B.J.E.). This research was also supported by the Agency of Science, Technology and Research (A*STAR; T.L.D.T.). We acknowledge the Integrated Molecular Structure Education and Research Center (IMSERC) for molecular characterization facilities for NMR spectroscopy supported by Northwestern U., the NSF under grants CHE-0923236 and CHE-9871268, Pfizer, and the State of Illinois. We also thank the Nanoscale Integrated Fabrication, Testing, and Instrument (NIFTI) and Keck Interdisciplinary Surface Science (KECK-II) facilities of Northwestern University's Atomic and Nanoscale Characterization Experimental (NUANCE) Center for UPS experiments, supported by Northwestern U., the State of Illinois, the Keck foundation, NSF-MRSEC, and NSF-NSEC. Finally, we thank Dr. Antonio Facchetti, J. T. Shin, and J. L. Song for helpful discussions.

REFERENCES

(1) Nyholm, L.; Nystrom, G.; Mihranyan, A.; Stromme, M. Toward Flexible Polymer and Paper-Based Energy Storage Devices. *Adv. Mater.* **2011**, *23*, 3751−3769.

(2) Mahapatra, S. S.; Yadav, S. K.; Yoo, H. J.; Cho, J. W. Highly Stretchable, Transparent and Scalable Elastomers with Tunable Dielectric Permittivity. *J. Mater. Chem.* **2011**, *21*, 7686−7691.

(3) Manceau, M.; Angmo, D.; Jorgensen, M.; Krebs, F. C. ITO-Free Flexible Polymer Solar Cells: From Small Model Devices to Roll-to-Roll Processed Large Modules. *Org. Electron.* **2011**, *12*, 566−574.

(4) Wolf, M. O.; Wrighton, M. S. Tunable Electron-Density at a Rhenium Carbonyl Complex Coordinated to the Conducting Polymer Poly[5,5′-(2-thienyl)-2,2′-bithiazole]. *Chem. Mater.* **1994**, *6*, 1526−1533.

(5) Dang, M. T.; Hirsch, L.; Wantz, G. P3HT:PCBM, Best Seller in Polymer Photovoltaic Research. *Adv. Mater.* **2011**, *23*, 3597−3602.

(6) Guo, X. G.; Zhou, N. J.; Lou, S. J.; Smith, J.; Tice, D. B.; Hennek, J. W.; Ortiz, R. P.; Navarrete, J. T. L.; Li, S. Y.; Strzalka, J.; Chen, L. X.; Chang, R. P. H.; Facchetti, A.; Marks, T. J. Polymer Solar Cells with Enhanced Fill Factors. *Nat. Photonics* **2013**, *7*, 825−833.

(7) Park, S. H.; Roy, A.; Beaupre, S.; Cho, S.; Coates, N.; Moon, J. S.; Moses, D.; Leclerc, M.; Lee, K.; Heeger, A. J. Bulk Heterojunction Solar Cells with Internal Quantum Efficiency Approaching 100%. *Nat. Photonics* **2009**, *3*, 297−303.

(8) Liang, Y. Y.; Xu, Z.; Xia, J. B.; Tsai, S. T.; Wu, Y.; Li, G.; Ray, C.; Yu, L. P. For the Bright Future-Bulk Heterojunction Polymer Solar Cells with Power Conversion Efficiency of 7.4%. *Adv. Mater.* **2010**, *22*, E135−E138.

(9) Burroughes, J. H.; Bradley, D. D. C.; Brown, A. R.; Marks, R. N.; Mackay, K.; Friend, R. H.; Burns, P. L.; Holmes, A. B. Light-Emitting-Diodes Based on Conjugated Polymers. *Nature* **1990**, *347*, 539−541.

(10) Han, T. H.; Lee, Y.; Choi, M. R.; Woo, S. H.; Bae, S. H.; Hong, B. H.; Ahn, J. H.; Lee, T. W. Extremely Efficient Flexible Organic Light-Emitting Diodes with Modified Graphene Anode. *Nat. Photonics* **2012**, *6*, 105−110.

(11) Liu, Y.; Liu, M. S.; Jen, A. K.-Y. Synthesis and Characterization of a Novel and Highly Efficient Light-Emitting Polymer. *Acta Polym.* **1999**, *50*, 105−108.

(12) Cheng, Y. J.; Liu, M. S.; Zhang, Y.; Niu, Y. H.; Huang, F.; Ka, J. W.; Yip, H. L.; Tian, Y. Q.; Jen, A. K. Y. Thermally Cross-Linkable Hole-Transporting Materials on Conducting Polymer: Synthesis, Characterization, and Applications for Polymer Light-Emitting Devices. *Chem. Mater.* **2008**, *20*, 413−422.

(13) Lee, J.; Kaake, L. G.; Cho, J. H.; Zhu, X. Y.; Lodge, T. P.; Frisbie, C. D. Ion Gel-Gated Polymer Thin-Film Transistors: Operating Mechanism and Characterization of Gate Dielectric Capacitance, Switching Speed, and Stability. *J. Phys. Chem. C* **2009**, *113*, 8972−8981.

(14) Sirringhaus, H.; Kawase, T.; Friend, R. H.; Shimoda, T.; Inbasekaran, M.; Wu, W.; Woo, E. P. High-Resolution Inkjet Printing of All-Polymer Transistor Circuits. *Science* **2000**, *290*, 2123−2126.

(15) Choi, W.; Harada, D.; Oyaizu, K.; Nishide, H. Aqueous Electrochemistry of Poly(vinylanthraquinone) for Anode-Active Materials in High-Density and Rechargeable Polymer/Air Batteries. *J. Am. Chem. Soc.* **2011**, *133*, 19839−19843.

(16) Song, Z.; Qian, Y.; Liu, X.; Zhang, T.; Zhu, Y.; Yu, H.; Otani, M.; Zhou, H. A Quinone Based Oligomeric Lithium Salt for Superior Li-Organic Battery. *Energy Environ. Sci.* **2014**, DOI: 10.1039/C4EE02575J.

(17) Zhu, L. M.; Niu, Y. J.; Cao, Y. L.; Lei, A. W.; Ai, X. P.; Yang, H. X. n-Type Redox Behaviors of Polybithiophene and Its Implications for Anodic Li and Na Storage Materials. *Electrochim. Acta* **2012**, *78*, 27−31.
(18) Liu, G.; Xun, S. D.; Vukmirovic, N.; Song, X. Y.; Olalde-Velasco, P.; Zheng, H. H.; Battaglia, V. S.; Wang, L. W.; Yang, W. L. Polymers with Tailored Electronic Structure for High Capacity Lithium Battery Electrodes. *Adv. Mater.* **2011**, *23*, 4679−4683.
(19) Wu, M. Y.; Xiao, X. C.; Vukmirovic, N.; Xun, S. D.; Das, P. K.; Song, X. Y.; Olalde-Velasco, P.; Wang, D. D.; Weber, A. Z.; Wang, L. W.; Battaglia, V. S.; Yang, W. L.; Liu, G. Toward an Ideal Polymer Binder Design for High-Capacity Battery Anodes. *J. Am. Chem. Soc.* **2013**, *135*, 12048−12056.
(20) Xun, S. D.; Song, X. Y.; Battaglia, V.; Liu, G. Conductive Polymer Binder-Enabled Cycling of Pure Tin Nanoparticle Composite Anode Electrodes for a Lithium-Ion Battery. *J. Electrochem. Soc.* **2013**, *160*, A849−A855.
(21) Etacheri, V.; Marom, R.; Elazari, R.; Salitra, G.; Aurbach, D. Challenges in the Development of Advanced Li-Ion Batteries: A Review. *Energy Environ. Sci.* **2011**, *4*, 3243−3262.
(22) Goodenough, J. B. Evolution of Strategies for Modern Rechargeable Batteries. *Acc. Chem. Res.* **2013**, *46*, 1053−1061.
(23) Goodenough, J. B.; Kim, Y. Challenges for Rechargeable Li Batteries. *Chem. Mater.* **2010**, *22*, 587−603.
(24) Larcher, D.; Beattie, S.; Morcrette, M.; Edstroem, K.; Jumas, J. C.; Tarascon, J. M. Recent Findings and Prospects in the Field of Pure Metals as Negative Electrodes for Li-Ion Batteries. *J. Mater. Chem.* **2007**, *17*, 3759−3772.
(25) Zhang, W. J. A Review of the Electrochemical Performance of Alloy Anodes for Lithium-Ion Batteries. *J. Power Sources* **2011**, *196*, 13−24.
(26) Aurbach, D.; Gamolsky, K.; Markovsky, B.; Salitra, G.; Gofer, Y.; Heider, U.; Oesten, R.; Schmidt, M. The Study of Surface Phenomena Related to Electrochemical Lithium Intercalation into Li_xMO_y Host Materials (M = Ni, Mn). *J. Electrochem. Soc.* **2000**, *147*, 1322−1331.
(27) Xu, K.; von Cresce, A. Interfacing Electrolytes with Electrodes in Li Ion Batteries. *J. Mater. Chem.* **2011**, *21*, 9849−9864.
(28) Verma, P.; Maire, P.; Novak, P. A Review of the Features and Analyses of the Solid Electrolyte Interphase in Li-Ion Batteries. *Electrochim. Acta* **2010**, *55*, 6332−6341.
(29) Zhang, D.; Haran, B. S.; Durairajan, A.; White, R. E.; Podrazhansky, Y.; Popov, B. N. Studies on Capacity Fade of Lithium-Ion Batteries. *J. Power Sources* **2000**, *91*, 122−129.
(30) Lange, I.; Blakesley, J. C.; Frisch, J.; Vollmer, A.; Koch, N.; Neher, D. Band Bending in Conjugated Polymer Layers. *Phys. Rev. Lett.* **2011**, *106*, 216402.
(31) Lange, I.; Kniepert, J.; Pingel, P.; Dumsch, I.; Allard, S.; Janietz, S.; Scherf, U.; Neher, D. Correlation between the Open Circuit Voltage and the Energetics of Organic Bulk Heterojunction Solar Cells. *J. Phys. Chem. Lett.* **2013**, *4*, 3865−3871.
(32) Lee, J. H.; Shin, J. H.; Song, J. Y.; Wang, W. F.; Schlaf, R.; Kim, K. J.; Yi, Y. Interface Formation between ZnO Nanorod Arrays and Polymers (PCBM and P3HT) for Organic Solar Cells. *J. Phys. Chem. C* **2012**, *116*, 26342−26348.
(33) Djurovich, P. I.; Mayo, E. I.; Forrest, S. R.; Thompson, M. E. Measurement of the Lowest Unoccupied Molecular Orbital Energies of Molecular Organic Semiconductors. *Org. Electron.* **2009**, *10*, 515−520.
(34) Chen, E. S.; Chen, E. C. M.; Sane, N.; Talley, L.; Kozanecki, N.; Shulze, S. Classification of Organic Molecules to Obtain Electron Affinities from Half Wave Reduction Potentials: The Aromatic Hydrocarbons. *J. Chem. Phys.* **1999**, *110*, 9319−9329.
(35) D'Andrade, B. W.; Datta, S.; Forrest, S. R.; Djurovich, P.; Polikarpov, E.; Thompson, M. E. Relationship between the Ionization and Oxidation Potentials of Molecular Organic Semiconductors. *Org. Electron.* **2005**, *6*, 11−20.
(36) Cardona, C. M.; Li, W.; Kaifer, A. E.; Stockdale, D.; Bazan, G. C. Electrochemical Considerations for Determining Absolute Frontier Orbital Energy Levels of Conjugated Polymers for Solar Cell Applications. *Adv. Mater.* **2011**, *23*, 2367−2371.
(37) Pavlishchuk, V. V.; Addison, A. W. Conversion Constants for Redox Potentials Measured Versus Different Reference Electrodes in Acetonitrile Solutions at 25°C. *Inorg. Chim. Acta* **2000**, *298*, 97−102.
(38) Bard, A. J.; Faulkner, L. R. *Electrochemical Methods: Fundamentals and Applications*, 2nd ed.; John Wiley & Sons: New York, 2001.
(39) Hou, J. H.; Tan, Z. A.; Yan, Y.; He, Y. J.; Yang, C. H.; Li, Y. F. Synthesis and Photovoltaic Properties of Two-Dimensional Conjugated Polythiophenes with Bi(thienylenevinylene) Side Chains. *J. Am. Chem. Soc.* **2006**, *128*, 4911−4916.
(40) Mccullough, R. D.; Williams, S. P. Toward Tuning Electrical and Optical-Properties in Conjugated Polymers Using Side-Chains: Highly Conductive Head-to-Tail, Heteroatom-Functionalized Polythiophenes. *J. Am. Chem. Soc.* **1993**, *115*, 11608−11609.
(41) Blouin, N.; Michaud, A.; Leclerc, M. A Low-Bandgap Poly(2,7-carbazole) Derivative for Use in High-Performance Solar Cells. *Adv. Mater.* **2007**, *19*, 2295−2300.
(42) Chen, Z. H.; Zheng, Y.; Yan, H.; Facchetti, A. Naphthalenedicarboximide- vs Perylenedicarboximide-Based Copolymers. Synthesis and Semiconducting Properties in Bottom-Gate N-Channel Organic Transistors. *J. Am. Chem. Soc.* **2009**, *131*, 8−9.
(43) Anderson, P. A. The Work Function of Lithium. *Phys. Rev.* **1949**, *75*, 1205−1207.
(44) Schroeder, P. G.; France, C. B.; Park, J. B.; Parkinson, B. A. Orbital Alignment and Morphology of Pentacene Deposited on Au(111) and SnS_2 Studied Using Photoemission Spectroscopy. *J. Phys. Chem. B* **2003**, *107*, 2253−2261.
(45) Yi, Y.; Lyon, J. E.; Beerbom, M. M.; Schlaf, R. Characterization of Indium Tin Oxide Surfaces and Interfaces Using Low Intensity X-Ray Photoemission Spectroscopy. *J. Appl. Phys.* **2006**, *100*, 093719.
(46) Song, C. K.; White, A. C.; Zeng, L.; Leever, B. J.; Clark, M. D.; Emery, J. D.; Lou, S. J.; Timalsina, A.; Chen, L. X.; Bedzyk, M. J.; Marks, T. J. Systematic Investigation of Organic Photovoltaic Cell Charge Injection/Performance Modulation by Dipolar Organosilane Interfacial Layers. *ACS Appl. Mater. Interfaces* **2013**, *5*, 9224−9240.
(47) Ciszkowska, M.; Osteryoung, J. G. Voltammetry of Metals at Mercury Film Microelectrodes in the Absence and the Presence of Varying Concentrations of Supporting Electrolyte. *Anal. Chem.* **1995**, *67*, 1125−1131.
(48) Lindstrom, H.; Sodergren, S.; Solbrand, A.; Rensmo, H.; Hjelm, J.; Hagfeldt, A.; Lindquist, S. E. Li^+ Ion Insertion in TiO_2 (anatase). 2. Voltammetry on Nanoporous Films. *J. Phys. Chem. B* **1997**, *101*, 7717−7722.
(49) Daum, P.; Murray, R. W. Charge-Transfer Diffusion Rates and Activity Relationships during Oxidation and Reduction of Plasma-Polymerized Vinylferrocene Films. *J. Phys. Chem.* **1981**, *85*, 389−396.
(50) Kadish, K. M.; Morrison, M. M. Solvent and Substituent Effects on the Redox Reactions of Para-Substituted Tetraphenylporphyrin. *J. Am. Chem. Soc.* **1976**, *98*, 3326−3328.
(51) Sawyer, D. T.; Chlericato, G.; Angelis, C. T.; Nanni, E. J.; Tsuchiya, T. Effects of Media and Electrode Materials on the Electrochemical Reduction of Dioxygen. *Anal. Chem.* **1982**, *54*, 1720−1724.
(52) Eslami, M.; Zare, H. R.; Namazian, M. The Effect of Solvents on the Electrochemical Behavior of Homogentisic Acid. *J. Electroanal. Chem.* **2014**, *720−721*, 76−83.
(53) Fleischmann, M.; Hendra, P. J.; Mcquilla, A. J. Raman-Spectra of Pyridine Adsorbed at a Silver Electrode. *Chem. Phys. Lett.* **1974**, *26*, 163−166.
(54) Andreas, H. A.; Conway, B. E. Examination of the Double-Layer Capacitance of an High Specific-Area C-cloth Electrode as Titrated from Acidic to Alkaline pHs. *Electrochim. Acta* **2006**, *51*, 6510−6520.
(55) Isse, A. A.; Gennaro, A. Absolute Potential of the Standard Hydrogen Electrode and the Problem of Interconversion of Potentials in Different Solvents. *J. Phys. Chem. B* **2010**, *114*, 7894−7899.
(56) Trasatti, S. The "Absolute" Electrode Potential—The End of the Story. *Electrochim. Acta* **1990**, *35*, 269−271.

(57) Trasatti, S. The Absolute Electrode Potential: An Explanatory Note (Recommendations 1986). *Pure Appl. Chem.* **1986**, *58*, 955−966.